Dorsal Anterior Cingulate Cortex Encodes the Subjective Motivational Value of Cognitive Task Performance

[a]Debbie M. Yee[1,2*], Jennifer L. Crawford[1], Todd S. Braver[1]

[1]Psychological and Brain Sciences, Washington University in St. Louis, St. Louis, MO, 63130, USA

[2]Cognitive, Linguistic, and Psychological Sciences, Brown University, Providence, RI, 02906, USA

*Correspondence : debbie_yee@brown.edu

[a]Lead Contact

Summary

Humans can seamlessly combine value signals from diverse motivational incentives, yet it is not well-understood how these signals are "bundled" in the brain to modulate cognitive control. The dorsal anterior cingulate cortex (dACC) is theorized to integrate motivational value dimensions in the service of goal-directed action, though this hypothesis has yet to receive rigorous confirmation. Here, we examine the role of dACC in motivational integration using an experimental paradigm that quantifies combined effects of liquid (e.g., juice, neutral, saltwater) and monetary incentives on cognitive task performance. These incentives modulated dACC activity in both a trial-by-trial and block-wise fashion. Incentive-related dACC modulation predicted fluctuations in cognitive performance and self-report motivation ratings. Statistical mediation analyses indicate that dACC encodes incentives in terms of subjective motivational value, and that this value signal is associated with task performance. These results suggest dACC integrates motivational signals to compute the expected value of goal-directed cognitive control.

Keywords: motivation, incentive integration, cognitive control, reward, value, dACC

Introduction

Motivational incentives play a central role in decision-making and the pursuit of behavioral and cognitive task goals (Botvinick and Braver, 2015). A particularly remarkable element of motivational influences on cognitive control is the ability to seamlessly integrate diverse incentives to modulate the allocation of cognitive resources towards pursuit of mentally demanding task goals. For example, when working towards completing a challenging project, a worker might be motivated by the potential promotion or raise they may receive, the positive social feedback their supervisor may provide, the tasty snack they promised themselves when the report is finished, or most likely, a combination of all of these incentives. Thus, the ability to integrate diverse incentives to modulate goal pursuit appears to be essential for normative cognitive function.

However, although it is intuitive that individuals likely combine, or "bundle" the values from multiple categories of incentives to influence their decision-making and goal pursuit (FitzGerald, Seymour and Dolan, 2009), prior studies of human motivation have almost exclusively examined the effects of monetary rewards (Kouneiher, Charron and Koechlin, 2009; Padmala and Pessoa, 2011; Bahlmann, Aarts and D'Esposito, 2015; Etzel *et al.*, 2015). Surprisingly few studies have explored the effects of nonmonetary and biologically relevant incentives (e.g., food, drink) on cognitive task performance (Krug and Braver, 2014). Yet consideration of primary and "bundled" incentives on cognition actually has strong theoretical relevance, by potentially clarifying the mechanisms by which value signals from different incentive categories are integrated in motivation-cognition interaction. In the current study, we directly test this idea and utilize fMRI measures of brain activity to elucidate the neural mechanisms that underlie this integrated motivational influence on cognitive control.

Several important existing theoretical frameworks provide relevant key predictions for the neural mechanisms underpinning incentive integration. One influential theory in neuroeconomics is the "common currency" account, which suggests that diverse goods and incentives are represented in a common neural representation that enables these goods to be compared, combined, and selected under decision-making contexts (Padoa-Schioppa, 2011; Levy and Glimcher, 2012). Moreover, the explicit encoding of such goods is thought to reflect a valuation process that enables individuals to rank order items in terms of their subjective utility or preference. One natural form for this utility encoding might be in terms of subjective motivational value, which has been speculated to be represented in ventromedial prefrontal cortex (vmPFC) and striatum (Chib *et al.*, 2009; Sescousse, Li and Dreher, 2015). Thus, the encoding of incentives in terms of subjective motivational value is also relevant for theories of motivation-cognition interaction, which suggests that cognitive control processes might be tightly coupled with motivational signals (Parro, Dixon and Christoff, 2018; Yee and Braver, 2018).

Another specific account is known as the Expected Value of Control (EVC) theory. This account suggests a primary role for the dorsal anterior cingulate cortex (dACC) in estimating the expected value of engaging cognitive control (Shenhav, Botvinick and Cohen, 2013; Shenhav *et al.*, 2017). In particular, the EVC account postulates that the dACC acts as a motivation-cognition hub, which integrates various sources of motivational value (i.e., costs and benefits) into a modulatory signal, which then specifies the allocation of cognitive control processes and adapts task performance accordingly (Shenhav, Cohen and Botvinick, 2016).

The EVC account is a compelling one, in postulating a privileged role for the dACC in the interface between motivation and cognition. The prior literature is broadly consistent with this account, as prior studies have demonstrated that dACC is reliably activated during incentivized

cognitive tasks (Parro, Dixon and Christoff, 2018), and engaged at the interface between incentive motivation and action selection (Rushworth *et al.*, 2004; Holroyd and Yeung, 2011; Heilbronner and Hayden, 2016). Critically, and most relevant to the current study, dACC also appears to be sensitive to both costs and benefits of engaging in cognitive control tasks (Sayalı and Badre, 2019; Westbrook, Lamichhane and Braver, 2019), as well as to both reward and punishment cues (Fujiwara *et al.*, 2009; Monosov, 2017; Lake *et al.*, 2019). Nevertheless, in order to provide a strong test of the claim that dACC serves as an integrative motivation-cognition hub, consistent with the EVC account, it is necessary to demonstrate that activity in this brain region: a) integrates the value of diverse incentives; b) integrates incentives with positive (i.e., appetitive) and negative (i.e., aversive) value; c) is directly associated with fluctuations in self-reported motivation; and d) that such motivational fluctuations are themselves linked with variation in cognitive task performance. A rigorous formal investigation of the mechanisms of incentive integration requires an experimental paradigm in which incentive values are bundled in a parametric manner, in order to measure how modulation across motivational variables relates to parametric changes in cognitive task performance. More importantly, the utilization of such a paradigm could provide unique and compelling insight into the neural mechanisms underpinning how diverse incentives may be combined (or "bundled") into an integrated motivational value signal and consequently modulate cognitive task performance.

In recent work, we have developed a novel task paradigm which provides a powerful investigative tool from which to test the hypothesis that dACC serves as a hub for the interface between motivation and cognitive control in the manner described above. In this incentive integration paradigm, liquid and monetary incentives are bundled together in a parametric manner in both a trial-by-trial and block-wise fashion, enabling estimation of how these incentives

modulate self-reported motivation and cognitive task performance. The incorporation of both liquid and monetary incentives is a critical feature of the paradigm, since the use of liquid incentives enable the straightforward and quantifiable manipulation of motivational valence through the use of positive/appetitive (juice), neutral (tasteless liquid), and negative/aversive (saltwater) liquids. Likewise, since participants directly consume and biologically process the liquids, they will likely value them according to subjective and idiosyncratic criteria (e.g., higher valuation of apple juice because of preference for sweet drinks). Such preferences may help further reveal their motivational influence on task performance (e.g., higher preference for apple juice may drive improved cognitive task performance). Our prior behavioral findings with this paradigm have demonstrated that the monetary and liquid incentives are additively combined in terms of their impact on self-reported motivation and task performance, and that these effects show a strong degree of individual variation as well (Yee *et al.*, 2016, 2019). In the current study, we adapt the incentive integration paradigm to a neuroimaging context, using fMRI to test the compatibility of observed dACC activity patterns during task performance with key claims of the EVC account.

This study addresses two critical questions. First, we investigate the neural mechanisms by which motivational values from primary and secondary incentives are integrated to modulate cognitive task performance. Specifically, we test whether activation in the dACC, a key area hypothesized to encode EVC, does in fact, reflect the integrated (i.e., "bundled") value of both incentive types. Second, we examine how such bundled neural value signals relate to incentive-driven modulations in cognitive task performance versus self-report measures of motivation. Importantly, we believe this novel study to be particularly innovative, as to our knowledge, it is the first human neuroimaging study to investigate how values from diverse incentives are combined into a putative integrated value neural signal to modulate cognitive task performance.

To preview, the results provide strong evidence that the dACC plays a central role in modulating the interaction between motivation and cognitive control, specifically via internal representation of the bundled motivational value signal that drives the allocation of cognitive control.

Results

Motivational Incentive Integration Effects: Reward Rate and Self-Reported Motivation Ratings

In the task, participants have the opportunity to earn monetary and liquid incentives on every trial if their performance is accurate and faster than a criterion RT cutoff (defined individually for each participant from their performance in a baseline condition). Consequently, we used the reward rate – defined as the percentage of trials in which the participant earned the available reward – as the primary dependent behavioral measure of motivated cognitive task performance. All participants (n=46) performed above the expected rate of 40%, indicating that they significantly improved their performance relative to baseline levels (45/46 participants showed statistically significant improvements in performance according to a binomial test; successes=117 trials=288, p=.05).

We found that different types of motivational incentives are integrated to modulate cognitive task performance. Specifically, we estimated a general linear mixed model with monetary reward and liquid valence as fixed effects with participant as a random effect. The model revealed significant effects of both monetary [b=.03, t=4.42, p<.001] and liquid incentives [b=.01, t=2.30, p=.022], but no significant interaction [b=.00, t=-.21, p=.830]. The liquid incentive effects were motivationally valenced, as expected by our prior work, in that performance was better when positive (juice) relative to negative (saltwater) liquids were offered as incentives. Post-hoc analyses further revealed a significant difference between neutral and saltwater [b=.03 t=2.12,

p=.034], but no significant effects between juice and neutral [b=.00, t=.08, p=.936]. Thus, the liquid effects on reward rates were primarily driven by impaired performance when saltwater was offered as incentive feedback (Figure 1B; although note that in our prior behavioral studies, we observed both performance facilitation effects due to juice, as well as performance impairments due to saltwater (Yee *et al.*, 2016, 2019; Crawford *et al.*, 2020)). Critically, the lack of interaction between incentives suggests a combined, additive effect on liquid incentives and monetary rewards on performance. Supplemental analyses of RT and accuracy revealed that reward rate improvements were primarily driven by a faster RT for higher monetary reward, but did not involve a speed-accuracy trade-off (See Tables S1 and S2).

Additionally, we found that self-report motivation ratings predicted unique variance in cognitive task performance beyond the experimental manipulation itself. Self-reported measures of motivation were collected for each of the 9 trial types (e.g., How motivated were you on Juice $ trials?) after task completion. A linear mixed effects model revealed these motivation ratings were significantly predicted by both monetary [b=.69, t=9.32, p<.001] and liquid incentives [b=.75, t=10.06, p<.001], such that participants reported more motivation for higher monetary reward and more appetitive liquid incentives (Figure 1C). We conducted a hierarchical regression to examine whether self-reported motivation predicted unique variance in reward rate over and above the experimentally manipulated motivational variables (See Supplemental Information). The hierarchical regression revealed that when self-reported motivation ratings were added to the model with experimental fixed effects (e.g., monetary reward, liquid valence), their inclusion increased predicted reward rate variance over and above the experimentally manipulated motivational variables [$\chi^2(3)=20.311$, p<.001]. These results suggest that self-reported fluctuations

in motivation are an important contributor to cognitive task performance in that they predict unique variance beyond the effects of monetary and liquid incentives.

Critically, the self-report findings suggest two key interpretations. First, participants could access their subjective motivational states. Second, although these subjective states were modulated by monetary and liquid incentives, the induced motivation from the incentives may have been a more proximal influence on task performance. That is, although both reward rate and self-report motivation ratings are sensitive to the incentive manipulations, the weak association between these metrics [r=.22, t(44)=1.541, p=.13] (See Figure 1D) suggests they might reflect overlapping yet dissociable motivational components of the incentivized cognitive task.

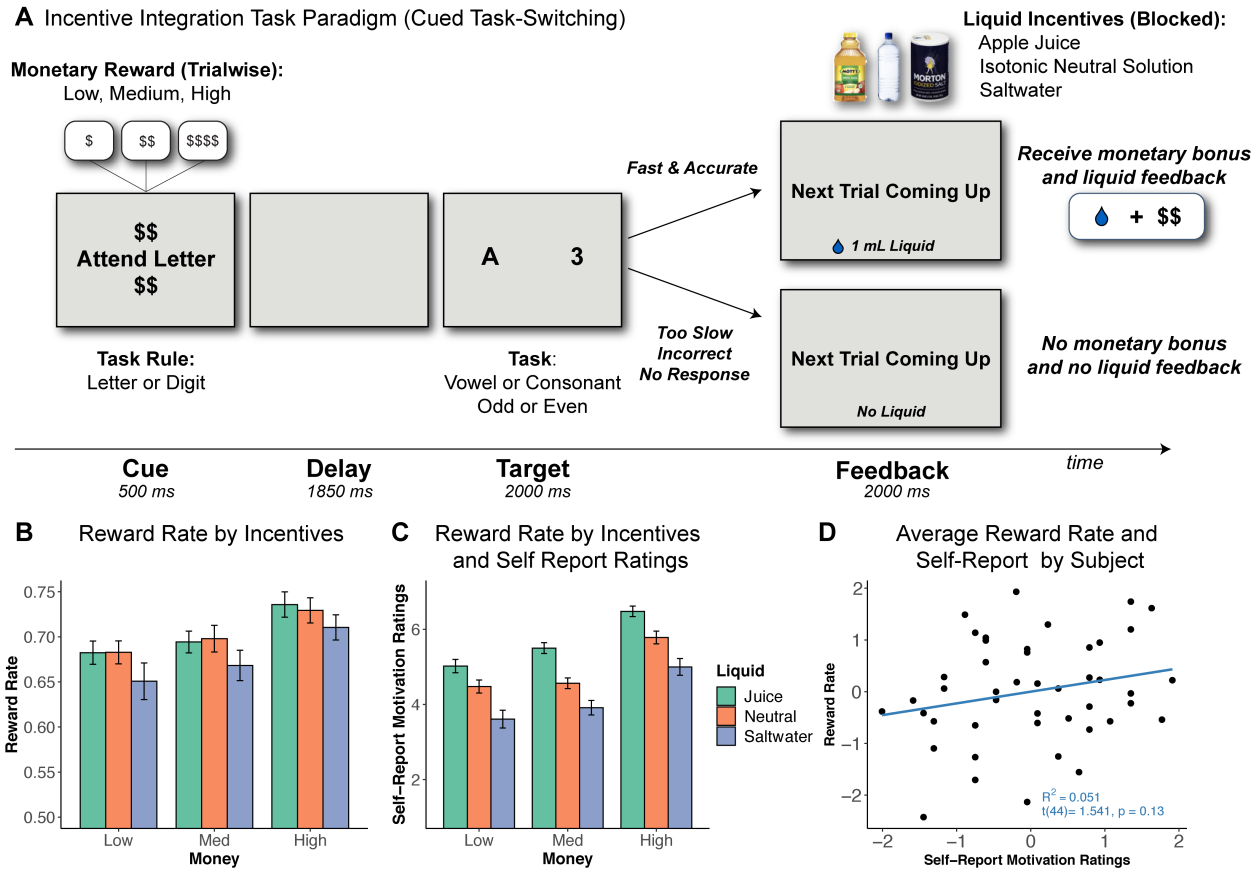

Figure 1: Incentive Integration Task Paradigm and Behavioral Results. A) Incentive integration task paradigm. Participants performed letter-digit cued task-switching and could earn monetary rewards and liquid incentives for accurate and fast performance (below an individualized criterion threshold). Notably, as the receipt of both monetary reward and liquid feedback was performance-contingent, participants had to integrate the value of both types of motivational

incentives when performing this cognitive task. **B)** Reward rate by motivational incentive conditions. Participants performed better with trials with higher monetary reward. In terms of liquid effects, participants performed worse on saltwater compared to juice or neutral trials. Error bars indicate SEM. **C)** Self-Report Motivation Ratings by motivational incentive conditions. Participants reported they were more motivated for higher monetary reward and more appetitive liquid incentives. Error bars indicate SEM. A hierarchical regression revealed that the inclusion of motivation ratings significantly predicted variance in reward rate beyond the experimental effects. **D)** Scatterplot of z-scored averaged reward rate and self-report motivation ratings by participant. Notably, although both measures are sensitive to the motivational incentive conditions, there was only a weak positive association between self-reported motivation and reward rate. These data suggest that the two measures reflect overlapping yet dissociable motivational components of the incentivized cognitive task.

Dorsal ACC Encodes Both Monetary and Liquid Incentives in Bundled Beta Estimates

We next focused on fMRI data to test whether dACC activity was predicted by monetary and liquid incentives. The dACC ROI encompasses the peak voxels of dACC based upon a prior meta-analysis on motivated cognitive control (Figure 2A), indicating that this ROI is consistently recruited during cognitive control tasks during which a reward incentive can be earned based upon task performance (Parro, Dixon and Christoff, 2018). For each participant, a general linear model was applied to extract beta estimates for sustained activation for each liquid block condition and event-related activation to the monetary incentive cues for each trial type (estimating activity 4-6 seconds after cue onset) using a deconvolved hemodynamic response function.

As predicted, our results revealed that dACC is sensitive to liquid valence via sustained responses and monetary reward via cue-related transient activation during each trial, which is consistent with the incentive delivery structure of the task paradigm and the duration of hemodynamic response lag. To first validate that dACC was independently sensitive to each incentive type, we conducted two linear mixed models with contrast coded monetary reward and liquid valence predicting the block and event-related cue beta estimates, respectively. The models revealed that the block beta estimates were predicted by liquid incentives [$b=.02$, $t=4.59$, $p<.001$]

but not monetary reward [b=0, t=0, p=1.000], whereas the cue beta estimates were predicted by monetary reward [b=.04, t=5.56, p<.001], but not liquid valence [b=0, t=-.31, p=.759]. Next, we "bundled" the beta estimates corresponding to the liquid incentive effects (blocked) and monetary reward effects (event-related, 4-6 seconds after cue onset), which enabled us to calculate 9 dACC bundled beta estimates for each participant corresponding to the 9 motivational conditions from the incentive integration task (e.g., $$-Juice, $$$$-Neutral; See Figure 2B). A critical assumption made was that summing the block and event-related beta estimate values would reflect the additive effects of both liquid and monetary incentives in the BOLD signal (i.e., the integrated value). This seems a plausible assumption, since the liquid effects were sustained throughout the task block, and thus by definition, available on every trial (i.e., to be added to the cue-triggered event-related activity). Importantly, the mixed model revealed that higher values of dACC bundled beta estimates were associated with higher monetary reward [b=.04, t=4.67, p<.001] and more appetitive liquid incentives [b=.02, t=2.98, p=.003], confirming that neural signals associated with primary and secondary incentives can be combined additively to represent the aggregate motivational value from both incentive types.

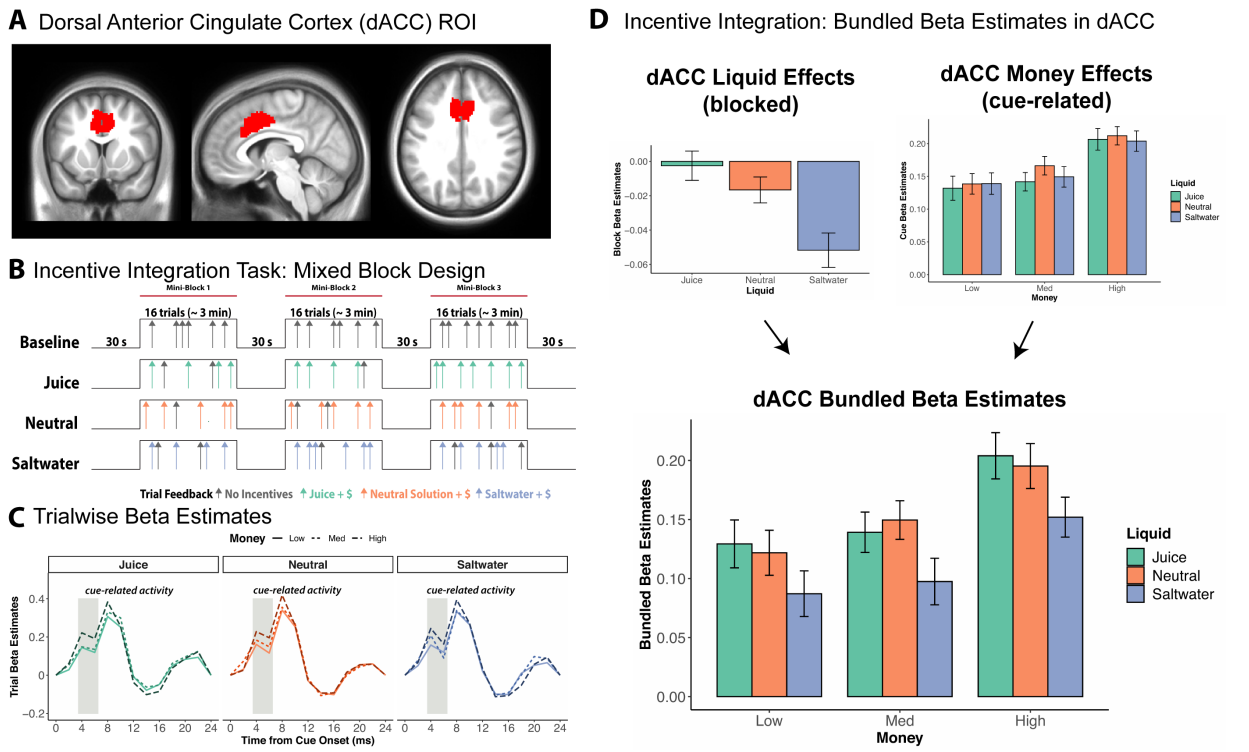

Figure 2: Dorsal ACC Encodes Both Monetary Rewards and Liquid Incentives in Bundled Beta Estimates. A) Bilateral dACC ROI mask. This ROI encompasses the peak voxels of dACC based upon a prior meta-analysis on motivated cognitive control (Parro, Dixon and Christoff, 2018). **B)** Mixed block/event-related design for incentive integration task. Participants performed 8 task blocks total, with two baseline blocks and six incentive blocks. Each participant's reward criterion (40%) was calculated based upon performance in the baseline run, and used to determine the RT threshold by which fast and accurate performance would lead to earned monetary and liquid incentives. Monetary reward value randomly varied on a trialwise basis. Liquid type was blocked and counterbalanced and delivered as performance feedback for successful attainment of monetary reward (shown in colored arrows). Participants did not receive money nor liquid for slow, incorrect, or abstained responses. A GLM was applied to extract the beta estimates for the sustained liquid block conditions and transient event-related motivation conditions for each participant (Petersen and Dubis, 2012). **C)** Trial wise beta estimates are illustrated for each of the 9 motivational incentive conditions. Darker colors indicate higher monetary reward level. Cue-related activity is highlighted in gray rectangles in each plot, demonstrating a significant monetary reward effect 4-6 seconds after cue onset. **D)** Bundled betas estimates in dACC are calculated by combining the beta estimates for sustained liquid effects and cue-related monetary reward effects from the event-related hemodynamic response. We assume an additive relationship between the monetary and liquid effects in terms of BOLD signal representation of integrated incentive value. Critically, reward rate was significantly predicted by dACC bundled betas, revealing that dACC represented the aggregate motivational value of primary and secondary incentives and is associated with parametric modulation of motivated cognitive task performance.

Reward Rate Predicted by Dorsal ACC Bundled Betas

Given the hypothesized role of dACC as a region that integrates various sources of motivational value into a modulatory signal that adaptively allocates cognitive control (i.e., as postulated by the EVC account; Shenhav et al., 2013), we aimed to test whether experimentally-manipulated within-subjects variability in dACC was significantly associated with similar within-subject variability in reward rate, our metric of motivated cognitive task performance. Such an association would provide compelling evidence demonstrating that dACC computes the aggregate value of both motivational incentives and predicts motivated task performance. We conducted a linear mixed effects model with reward rate predicted by dACC bundled beta estimates and 'incentive conditions' (contrast coded as the sum of liquid and monetary reward contrast codes). Importantly, our analyses revealed that reward rate was significantly predicted by both incentive conditions (as expected from prior analyses) [b=.02, t=2.91, p<.001] and dACC bundled betas [b=.09, t=2.41, p=.016]. A critical and important observation is that the inclusion of dACC bundled betas explained significant additional variation in reward rate beyond the experimentally-manipulated incentive effects, suggesting a role of dACC in encoding subjective motivational value. Moreover, these data are consistent with the EVC account of dACC as a hub for integrating value and cost information to derive an optimal control signal that balances task demands against potential rewards.

Self-Report Motivation Ratings Predicted by Dorsal ACC Bundled Betas

A secondary aim was to understand the putative relationship between the extent to which motivated cognitive task performance (i.e., reward rate) and self-reported motivation measures may be encoded in dACC activation. As self-report measures of motivation have been historically

viewed as the "gold standard" for assessing human motivational states (Hermans, 1970), we investigated the extent to which human dACC neural signals may encode self-reported motivation to exert cognitive control in order to maximize earnings of the bundled incentives. Here, we conducted a similar mixed model as above except now with self-report motivation ratings (rather than reward rate) as the dependent measure. Our analyses revealed that self-reported motivation ratings were predicted by both incentive condition [b=.67, t=9.78, p<.001] and dACC bundled betas [b=1.64, t=3.96, p<.001]. These results are particularly intriguing because this association reveals that dACC neural signals also reflect a subjective (and accurate) measure of the valuation of the bundled motivational incentives in the current task context. Moreover, such ratings may tap into a complementary motivation-related construct distinct from motivation associated with the exerted effort on a cognitively demanding task.

Dorsal ACC Effects on Reward Rate Mediated by Self-Report Motivation Ratings

Given the observed strong associations between dACC and reward rate, as well as between dACC and self-reported motivation ratings, we next examined the putative causal relationship between within-subjects variability across different incentive conditions in dACC, reward rate, and motivation ratings. In particular, given the utility of self-report ratings as a powerful metric for measuring subjective motivational states, we hypothesized that such ratings might partially explain the proximal motivational impact of the incentives on the associative modulatory relationship between dACC activity and reward rate. Such a within-subjects mediation would be compelling, as it would reveal the extent to which dACC may encode these two behavioral metrics as similar or distinct indices of an individual's current motivational state.

First, we conducted three linear mixed models and confirmed that experimentally manipulated incentives demonstrated quantifiable effects on within-subjects variability in dACC, reward rate, and self-report ratings. As indicated previously, incentive conditions significantly predicted dACC bundled betas [b=.03, t=4.04, p<.001], reward rate [b=.02, t=3.36, p<.001], and motivation ratings [b=.72, t=10.35 , p<.001]. (See red dashed lines in Figure 3). Critically, these data demonstrate that the incentive manipulations influence all three variables, while also suggesting that these motivational variables may be mediated or moderated by each other.

Next, we conducted a Bayesian multilevel mediation analysis and observed that incentive-modulated effects on the relationship between dACC and reward rate were mediated by such variability in motivation ratings, as prior linear mixed models confirmed incentive effects across all three variables. The within-subjects mediation analysis utilized averaged values across each of the nine possible motivational incentive conditions for each participant. This enabled us to compare within-subjects variability across incentive conditions between these variables (dACC, reward rate, motivation ratings). Importantly, this approach eliminated the need for including contrast-coded incentive effects in linear mixed models that were used to validate assumptions about associations between these variables prior to conducting the mediation analysis. Linear mixed models (without contrast-coded incentive effects) confirmed that dACC significantly predicted both reward rate [b=.14, t=3.77, p<.001] and motivation ratings [b=2.77, t=5.98, p<.001]. Moreover, in a linear mixed model of reward rate with motivation ratings as the mediator, controlling for the predictor revealed that motivation ratings significantly predicted reward rate [b=.02, t=5.53, p<.001], and more importantly, the inclusion of these ratings weakened the effect of dACC, though it still remained statistically significant [b=.08, t=2.15, p=.032]. Finally, these variables were submitted to a Bayesian multilevel mediation (using the bmlm package in R) to

estimate the medians and 95% credible intervals for the posterior distributions for each path parameter (See blue lines in Figure 3). The mediation analysis revealed that motivation ratings partially mediated the relationship between dACC and reward rate [mediated effect=.05, CI_{95}=(.00,.10); proportion mediated effect=.35, CI_{95}=(.04,1.04)], reducing the direct effect [c=.14, CI_{95}=(.04,.23); c'=.08, CI_{95}=(.00,.18)]. Thus, although dACC is significantly associated with incentive motivational task performance, this relationship is partially mediated by the variance explained by the self-report motivation ratings.

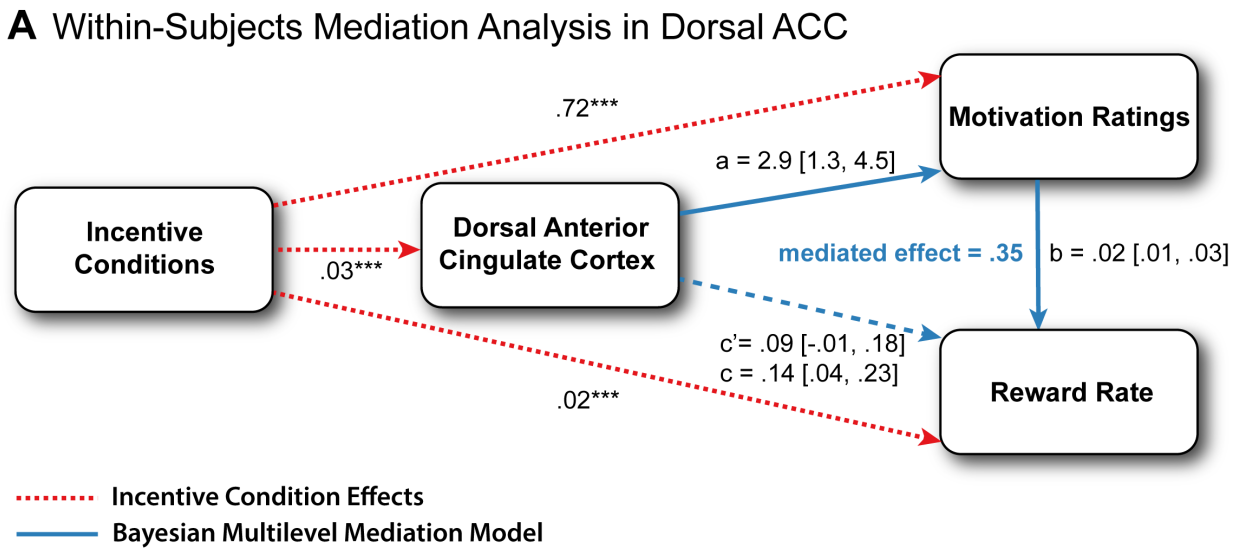

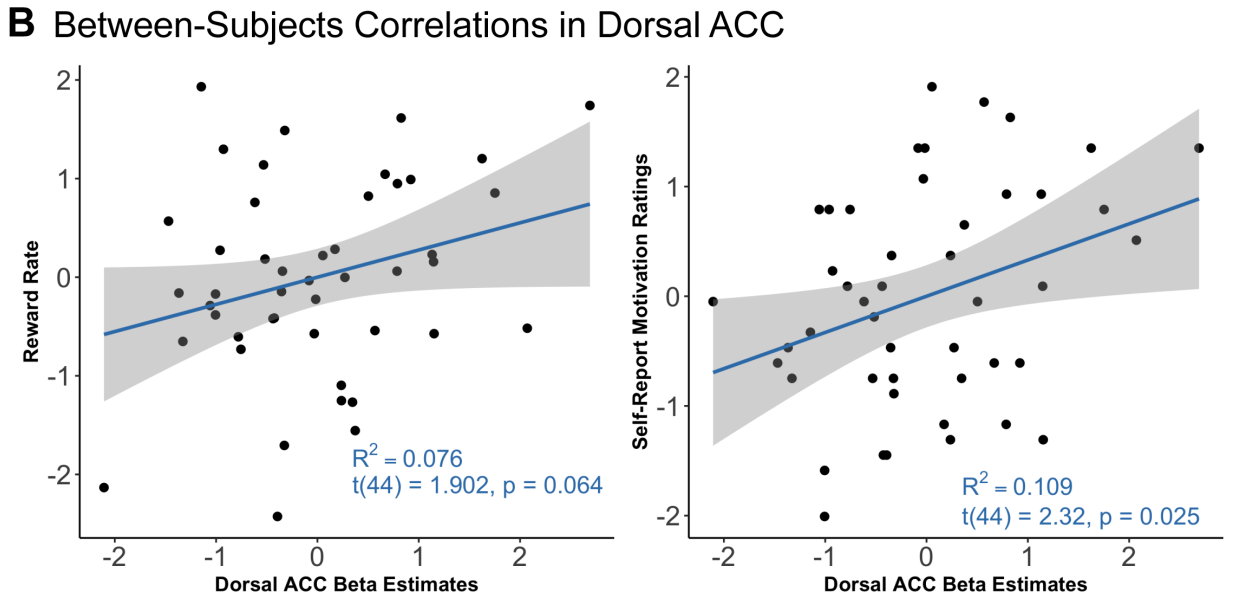

Figure 3: Dorsal ACC Effects on Reward Rate Mediated by Self-Report Motivation Ratings. A) Within-Subjects Mediation Analysis of Dorsal ACC. Three linear mixed effects models were conducted to confirm the effects of incentive conditions in dACC, reward rate, and motivation ratings (See red dashed lines). The models revealed that incentive conditions significantly predicted dACC bundled betas, reward rate, and motivation ratings. Next, a Bayesian multilevel within-subjects mediation analysis was conducted to test for a causal relationship between these three variables. The mediation analyses revealed that the relationship between within-subjects variability in dACC and reward rate was mediated by within-subjects variability in motivation ratings (See blue lines). Inclusion of motivation ratings partially mediated the association between dACC and reward rate (proportion mediated effect = .35, CI=[.04,1.04]). 95% credible intervals are used as the range of the posterior distribution for each of the path parameters. *p<.05; **p<.01; ***p<.001. **B)** Between-Subjects Correlations of Dorsal ACC. The left scatterplot of z-scored averaged dACC beta estimates and reward rate by subject revealed a weak association between dACC and reward rate. The right scatterplot shows z-scored averaged dACC beta estimates and self-report motivation ratings revealed a significant association between dACC and motivation ratings.

In addition to examining within-subjects variability, we also tested whether between-subjects' differences in dACC activation were associated with reward rate and motivation ratings. That is, if baseline differences in overall dACC activation across individuals correlated with reward rate and motivation ratings, it would suggest that dACC also reflects more stable levels of task engagement (between-subjects variability), beyond integrating task-related changes in incentive values towards motivated task performance (within-subjects variability). We averaged and normalized subject-level values for dACC activation, reward rate, and motivation ratings (i.e., rather than across the 9 incentive conditions). Our results revealed a weak association between dACC and reward rate [r=.28, t(44)=1.902, p=.064], but a significant association between dACC and motivation ratings [r=.33, t(44)=2.32, p=.025] (See Figure 3B). Individuals who reported higher overall motivation ratings (and to a lesser extent, higher reward rates) also showed a trend towards higher dACC activity. However, these between-subjects dACC effects were not as reliable as the within-subjects dACC effects previously demonstrated. In particular, when both subject-level dACC activity and motivation ratings were included in a model predicting subject-level

individual differences in average reward rate, neither variable was statistically reliable [dACC: b=.23, t=1.47, p=.149; Motivation Ratings: b=.15, t=.99, p=.328]. Thus, these data suggest that the dACC accurately encodes context-specific motivational states that are primarily modulated in a dynamic fashion (i.e., by incentive cues) rather than by more stable or global trait-like differences in motivation.

Dorsal ACC Selectively Encodes Subjective Motivational Value and Modulates Motivated Task Performance

Finally, we complemented our analyses of dACC activity patterns by examining other relevant brain regions of interest. In particular, a number of well-established brain regions have been implicated in value-based decision making (e.g., striatum, vmPFC), and other reward-related processes, such as taste processing (e.g., anterior insula). Consequently, we tested whether the subjective motivational value signal associated with task performance was also encoded in these other value-related brain regions. We conducted the same linear mixed models with reward rate and motivation ratings predicted by the motivational incentive conditions and bundled betas, except now using bundled betas from other regions of interest associated with value-based decision making (Bartra, McGuire and Kable, 2013; Sescousse *et al.*, 2013; Sescousse, Li and Dreher, 2015) as well as taste processing (Small, 2010). Of these selected ROIs, it is noteworthy that only dACC significantly predicted reward rate. In contrast, motivation ratings were additionally significantly predicted by caudate [b=.74, t=2.29, p=.022], putamen [b=1.29, t=3.22, p=.001], and anterior insula [b=1.36, t=2.87, p=.003] (See Figure 4). Critically, these data reveal that although several regions appear to predict motivation ratings (suggesting multiple brains regions may track the subjective motivation of the incentives), the specificity of the association between dACC and

reward rate robustly supports the EVC theory, i.e., that dACC may play a significant and selective role in modulating how motivational values are translated in effortful action during the performance of a cognitively demanding task.

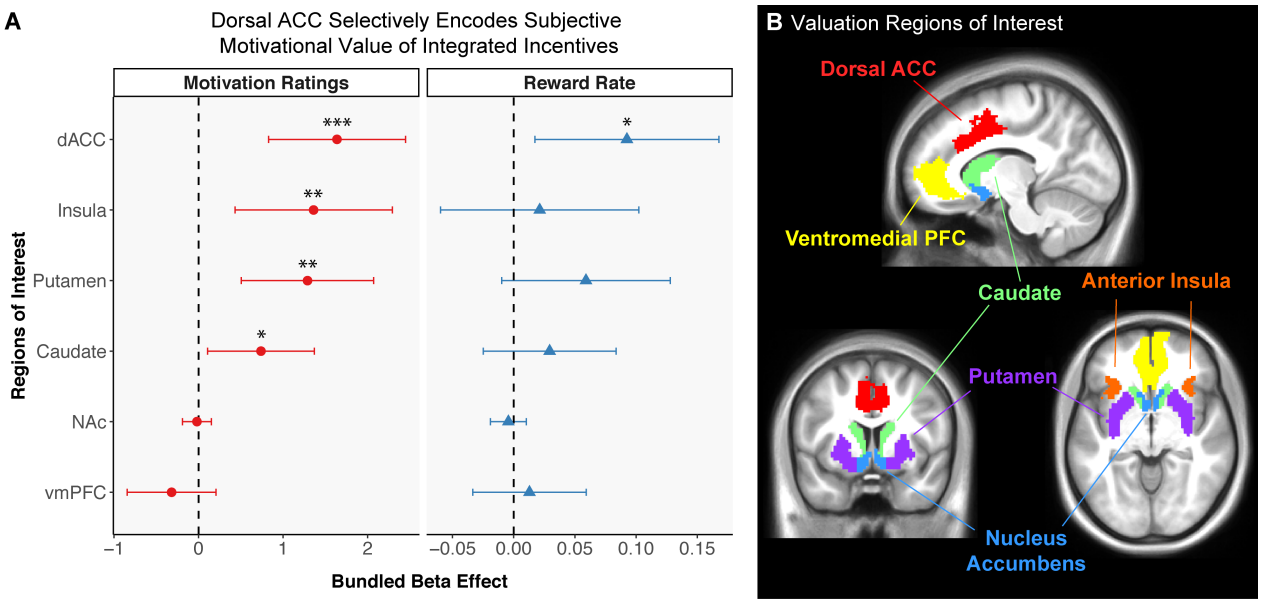

Figure 4: **Dorsal ACC Selectively Encodes Subjective Motivational Value and Modulates Motivated Task Performance. A)** To test for selectivity of dACC in motivational incentive integration, bundled beta estimates were calculated for *a priori* regions of interest associated with value-based decision-making (striatum, vmPFC) and taste processing (anterior insula). Mixed models were implemented with selected ROIs and plotted to compared to dACC effects on reward rate and motivation ratings. Error bars represent 95% confidence intervals. The right panel reveals that only dACC significantly predicted reward rate. The left panel reveals that motivation ratings were also significantly predicted anterior insula, caudate, and putamen, in addition to dACC, suggesting that self-reported motivation of incentives is encoded across multiple valuation brain regions. These data reveal the specificity of the relationship between dACC and reward rate, demonstrating that dACC encodes the translation of motivational value is transformed into effortful actions on a cognitively demanding task. *p<.05; **p<.01; ***p<.001. **B)** Visualization of valuation brain regions of interest.

Discussion

We found novel evidence that dACC represents the integrated subjective motivational value of bundled primary and secondary incentives, and moreover, that this bundled neural signal is selectively associated with changes in motivated cognitive task performance. Critically, these

findings provides clear support that dACC acts as integrative motivation-cognition hub, which combines signals of positive and negative incentive value towards computation of an output signal that allocates cognitive control in accordance with the expected motivational value of the current situational context. To obtain these results, we leveraged key features of our incentive integration paradigm, which enables estimation of the combined effect of both monetary and liquid incentives on brain activity and task performance, while also allowing for examination of motivational valence effects through the use of both appetitive and aversive liquid feedback. These findings are consistent with the broader literature and accounts postulating that dACC encodes the optimal allocation and deployment of control to accomplish cognitively effortful behavioral goals (Holroyd and Yeung, 2012; Shenhav *et al.*, 2017). Although some prior work has demonstrated the role of dACC in utilizing reward information to optimally allocate effort in rodents (Hosking, Cocker and Winstanley, 2014; Holroyd and McClure, 2015), ours is the first study to demonstrate the role of human dACC in encoding subjective motivational value across integrated incentives to modulate behavioral performance in a task with high cognitive demands.

A notable observation was the discovery that activity in the dACC was also associated with self-report motivation ratings, which is intriguing since these ratings explained unique variance in reward rate beyond the incentive manipulations. Additionally, these motivation ratings partially mediated the relationship between dACC and reward rate, providing suggestive evidence that such ratings may reflect the more proximal impact of the incentive conditions encoded in dACC activity. Moreover, the self-reported motivational effects of the incentive manipulations may be somewhat distinct, though functionally related to the types of motivational effects inferred from behavioral enhancements observed during incentivized task performance (Bonner and Sprinkle, 2002). Alternatively, these motivation ratings may simply reflect a more accurate subject-specific

indication of incentive salience based upon the ordinal levels from the manipulation. Future work should aim to investigate the extent to which both measures (i.e., motivated task performance, self-report) reflect convergent versus divergent neural signals underpinning motivation. Such clarification may reconcile discrepancies often observed between how these two measures (self-report, behavioral performance) reflect motivated cognition (Dang, King and Inzlicht, 2020). Moreover, such work could inform how distinct sources of motivational information are represented in the brain.

Interestingly, the incentive integration neural mechanism appears to be present in dACC, but not in other brain regions classically associated with representing the neural common currency of subjective value (Peters and Büchel, 2010; Levy and Glimcher, 2012). Nevertheless, our results are consistent with prior work that has shown a distinction between the subjective value signals associated with explicit economic choices (i.e., choosing one good over another) versus when values are relevant for behavioral actions (Camille, Tsuchida and Fellows, 2011; Cai and Padoa-Schioppa, 2012; Kolling *et al.*, 2016). In other words, the former process (value-based decision-making) involves explicit valuation and comparison of incentives, whereas the latter process (motivated cognitive control) involves implicit processing and utilization of incentive value for adaptive mobilization of cognitive control. Although a key feature of this study is the utilization of both monetary rewards and liquid incentives, our task design significantly deviates from prior neuroeconomic studies that have evaluated the expectation of primary and secondary incentives in humans (Chib *et al.*, 2009; Kim, Shimojo and O'Doherty, 2011; Park *et al.*, 2011; Sescousse *et al.*, 2013; Zhang *et al.*, 2017).

Most prior evidence supporting the neural common currency account arises from human and animal studies in which there is an explicit valuation phrase or when an economic choice is

required between available goods or options (Padoa-Schioppa and Conen, 2017; Frömer, Wolf and Shenhav, 2019). Because our current task paradigm is optimized for motivated cognitive control, it is unsurprising that only dACC neural signals appeared to encode the incentive condition effects on reward rate. Intriguingly, these results are consistent with prior work demonstrating that cost-benefit valuation in physical effort tasks elicit activation in dACC, but not vmPFC (Croxson *et al.*, 2009; Klein-Flügge *et al.*, 2016). Furthermore, this distinction between value-based decision making and motivated cognitive control is additionally supported by our observation that motivation ratings were associated with bundled betas in dorsal striatum (e.g., caudate, putamen), a region well-known to be associated with motivated action selection and control (Balleine, Delgado and Hikosaka, 2007; Balleine and O'Doherty, 2010; Miller *et al.*, 2014).

Future work should aim to bridge the gap between motivated cognitive control and value-based decision-making. One way to accomplish this would be to extend the paradigm, with an additional valuation phase for bundled incentives (e.g., $$$$ reward + saltwater), as well as a decision-making component in which choice preferences can be expressed between bundled incentives (e.g., $$$$ reward + saltwater vs. $$ reward + juice). Such a modification would enable comparison of the neural mechanisms that underlie explicit valuation and choice between incentives (economic decision-making) and implicit valuation of incentives for task performance (motivated cognition and control). We hypothesize that this type of paradigm might more clearly reveal a double dissociation for regions involved in explicit incentive valuation (e.g., vmPFC, ventral striatum) versus the utilization of motivational incentive value to modulate adaptive recruitment of cognitive control to accomplish behavioral task goals (e.g., dACC, dorsal striatum).

Additionally, a broader question raised in this study relates to developing a mechanistic understanding of how dACC integrates incentive values during motivated cognitive control. It is

well-known that dACC contains a heterogeneous population of neurons and underpins a diverse array of cognitive, motor, and affective functions (Bush *et al.*, 2002; Heilbronner and Hayden, 2016; Vega *et al.*, 2016). However, in light of our key findings supporting the role of dACC as a hub for motivation-cognition interactions (Parro, Dixon and Christoff, 2018), the precise calculations by which different neurons, voxels, or sub-regions within the dACC perform incentive value integration remains to be elucidated. One possibility is that distinct neural patterns or voxel clusters within dACC may have distinct functions in terms of encoding positive outcomes (e.g., monetary rewards, appetitive juice) versus negative outcomes (e.g., punishments, aversive saltwater). Such patterns seem plausible, given recent work demonstrating that dACC neurons respond to rewards and punishments in nonhuman primates (Monosov, 2017) and rodents (Schneider *et al.*, 2020). Alternatively, dACC voxels may be multiplexed to encode both positive and negative outcomes, or even incentives and actions (Hayden and Platt, 2010), depending on the specific context. Thus, an important future direction would be investigation with higher spatial resolution the boundary conditions related to when and how dACC integrates diverse incentives to represent the subjective motivational value in cognitive control contexts.

Finally, developing greater insight into how incentive motivation is integrated and represented in the brain may inform additional important aspects of how subjective value signals modulate task representations in prefrontal cortex (PFC). Whereas prior work has shown that lateral PFC signals are enhanced when higher monetary rewards are present (Kouneiher, Charron and Koechlin, 2009; Dixon and Christoff, 2012; Bahlmann, Aarts and D'Esposito, 2015; Duverne and Koechlin, 2017), how such cognitive task PFC representations interface with the subjective motivational value computation in dACC remains an open question. A promising future direction would be to exploit multivariate analyses (e.g., decoding or representational similarity analysis) to

better probe how value signals are integrated (in dACC) to modulate neural representations of cognitive task rules (in lateral PFC) and ultimately translated to measurable changes in behavior (Etzel *et al.*, 2015; Wisniewski *et al.*, 2015). Importantly, such findings would provide a more comprehensive understanding of systems-level neural representations of how diverse motivational incentives combine into subjective motivational value to support the pursuit of cognitive task goals.

Broadly, given the diversity of incentives that people encounter on a daily basis (e.g., social rewards), an open question relates to the challenge of how people evaluate and integrate multiple diverse types of incentives in the real world (Lehner *et al.*, 2017). Thus, our innovative approach lays the critical foundation for more careful study of real-world effort allocation, through which incentives vary along several types (e.g., monetary, liquid, social) and dimensions (e.g., appetitive, aversive), and are seamlessly integrated (e.g., consideration of both monetary rewards and social praise (Park *et al.*, 2018; Crawford *et al.*, 2020)). Importantly, such insight into the neural mechanisms underpinning how motivational incentives are integrated to modulate effortful tasks can also provide a mechanistic framework that can advance understanding of how such mechanisms become maladaptive in clinical disorders associated with motivational or cognitive deficits. (e.g., anxiety, depression (Huang *et al.*, 2015; Grahek *et al.*, 2019))

Acknowledgments

We would like to thank Carolyn Dean Wolf, Katherine Shapiro, and Bidhan Lamichhane for their assistance with data collection and technical support. We also thank Amitai Shenhav, Katherine Conen, and the CCP and Shenhav labs for helpful discussions during manuscript preparation. The research was supported by the National Institutes Health (R21-AG058206, R21-AG067295 to T.S.B. and subaward R24-AG054355 D.M.Y.) and McDonnell Center for Systems Neuroscience (T.S.B. and D.M.Y.). D.M.Y. and J.L.C. were supported by T32-AG000030, and D.M.Y. was additionally supported by F31-DA042574 and T32-NS073547.

Author Contributions

Conceptualization, D.M.Y. and T.S.B.; Methodology, D.M.Y. and T.S.B.; Investigation, D.M.Y and J.L.C.; Formal Analysis, D.M.Y.; Writing – Original Draft, D.M.Y.; Writing –Review & Editing, D.M.Y. J.L.C., and T.S.B.; Funding Acquisition, T.S.B. and D.M.Y.; Supervision, T.S.B.

Declaration of Interests

The authors declare no competing interests.

Figure 1: Incentive Integration Task Paradigm and Behavioral Results. A) Incentive integration task paradigm. Participants performed letter-digit cued task-switching and could earn monetary rewards and liquid incentives for fast and accurate performance (below a subjective criterion threshold). Notably, as the receipt of both monetary reward and liquid feedback was performance-contingent, participants had to integrate the value of both types of motivational incentives when performing this cognitive task. **B)** Reward rate by motivational incentive conditions. Participants performed better with trials with higher monetary reward. In terms of liquid effects, participants performed worse on saltwater compared to juice or neutral trials. Error bars indicate SEM. **C)** Self-Report Motivation Ratings by motivational incentive conditions. Participants reported they were more motivated for higher monetary reward and more appetitive liquid incentives. Error bars indicate SEM. A hierarchical regression revealed that the inclusion of motivation ratings significantly predicted variance in reward rate beyond the experimental effects. **D)** Scatterplot of z-scored averaged reward rate and self-report motivation ratings by participant. Notably, although both measures are sensitive to the motivational incentive conditions, there was only a weak positive association between self-reported motivation and reward rate. These data suggest that the two measures reflect overlapping yet dissociable motivational components of the incentivized cognitive task.

Figure 2: Dorsal ACC Encodes Both Monetary Rewards and Liquid Incentives in Bundled Beta Estimates. A) Bilateral dACC ROI mask. This ROI encompasses the peak voxels of dACC based upon a prior meta-analysis on motivated cognitive control (Parro, Dixon and Christoff, 2018). **B)** Mixed block/event-related design for incentive integration task. Participants performed 8 task blocks total, with two baseline blocks and six incentive blocks. Each participant's reward criterion (40%) was calculated based upon performance in the baseline run, and used to determine the RT threshold by which fast and accurate performance would lead to earned monetary and liquid incentives. Monetary reward value randomly varied on a trialwise basis. Liquid type was blocked and counterbalanced and delivered as performance feedback for successful attainment of monetary reward (shown in colored arrows). Participants did not receive money nor liquid for slow, incorrect, or abstained responses. A GLM was applied to extract the beta estimates for the sustained liquid block conditions and transient event-related motivation conditions for each participant (Petersen and Dubis, 2012). **C)** Trial wise beta estimates are illustrated for each of the 9 motivational incentive conditions. Darker colors indicate higher monetary reward level. Cue-related activity is highlighted in gray rectangles in each plot, demonstrating a significant monetary reward effect 4-6 seconds after cue onset. **D)** Bundled betas estimates in dACC are calculated by combining the beta estimates for sustained liquid effects and cue-related monetary reward effects from the event-related hemodynamic response. We assume an additive relationship between the monetary and liquid effects in terms of BOLD signal representation of integrated incentive value. Critically, reward rate was significantly predicted by dACC bundled betas, revealing that dACC represented the aggregate motivational value of primary and secondary incentives and is associated with parametric modulation of motivated cognitive task performance.

Figure 3: Dorsal ACC Effects on Reward Rate Mediated by Self-Report Motivation Ratings. A) Within-Subjects Mediation Analysis of Dorsal ACC. Three linear mixed effects models were conducted to confirm effects of incentive conditions in dACC, reward rate, and motivation ratings (See red dashed lines). The models revealed that incentive conditions significantly predicted dACC bundled betas, reward rate, and motivation ratings. Next, a Bayesian multilevel within-subjects mediation analysis was conducted to test for a causal relationship between these three variables. The mediation analyses revealed that the relationship between within-subjects variability in dACC and reward rate was mediated by within-subjects variability in motivation ratings (See blue lines). Inclusion of motivation ratings partially mediated the association between dACC and reward rate (proportion mediated effect = .35, CI=[.04,1.04]). 95% credible intervals are used as the range of the posterior distribution for each of the path parameters. *p<.05; **p<.01; ***p<.001. **B)** Between-Subjects Correlations of Dorsal ACC. The left scatterplot of z-scored averaged dACC beta estimates and reward rate by subject revealed a weak association between dACC and reward rate. The right scatterplot shows z-scored averaged dACC beta estimates and self-report motivation ratings revealed a significant association between dACC and motivation ratings.

Figure 4: **Dorsal ACC Selectively Encodes Subjective Motivational Value and Modulates Motivated Task Performance. A)** To test for selectivity of dACC in motivational incentive integration, bundled beta estimates were calculated for *a priori* regions of interest associated with value-based decision-making (striatum, vmPFC) and taste processing (anterior insula). Mixed models were implemented with selected ROIs and plotted to compared to dACC effects on reward rate and motivation ratings. Error bars represent 95% confidence intervals. The right panel reveals that only dACC significantly predicted reward rate. The left panel reveals that motivation ratings were also significantly predicted anterior insula, caudate, and putamen, in addition to dACC, suggesting that self-reported motivation of incentives is encoded across multiple valuation brain regions. These data reveal the specificity of the relationship between dACC and reward rate, demonstrating that dACC encodes the translation of motivational value is transformed into effortful actions on a cognitively demanding task. *p<.05; **p<.01; ***p<.001. **B)** Visualization of valuation brain regions of interest.

Figure S1: Response Time and Accuracy for each of the 9 Experimental Task Conditions. **A)** Response Time by 9 motivational incentive conditions. **B)** Accuracy by 9 motivational incentive conditions. Errors bars indicate 95% confidence intervals.

Figure S2: Self-Reported Liking and Intensity Ratings for Each Liquid. A) Participants reported significantly different and transitive liquid preferences (Juice > Neutral > Saltwater). B) Participants reported juice and saltwater as more intense than neutral.

Table S1: Response times and accuracy mixed model by monetary reward and liquid incentives.

STAR Methods

RESOURCE AVAILABILITY

Lead Contact

Further information and requests for MRI neuroimaging data, task scripts, and analysis scripts, should be directed to and will be fulfilled by the Lead Contact, Debbie Yee (debbie_yee@brown.edu).

Materials Availability

The study did not generate unique reagents.

Data and Code Availability

The behavioral data and analyses scripts are available on OSF: https://osf.io/upka4/. MRI data are available upon request.

EXPERIMENTAL PROCEDURES

Participants

51 right-handed participants (25 female; 18-38 years, M=25.1, SD=4.8) with normal or corrected-to-normal vision participated in the experiment. All participants provided written consent approved by the Washington University Institutional Review Board, and received payment for their participation ($25 per hour), plus additional earnings of up to 15 dollars based on task performance. Five participants were excluded from analyses due to technical error, participant inability to complete the task, or participant noncompliance with task instructions. The final sample consisted of 46 participants (22 females; 18–38 years, M=25.4, SD=4.9). All demographic

and self-report data were collected and managed using a secure web-based application, Research Electronic Data Capture (REDCap), hosted at Washington University (Harris *et al.*, 2009).

Incentive Integration Task

To examine the dissociable and bundled effects of primary and secondary incentives on cognitive control, we adapted the consonant-vowel odd-even (CVOE) cued task-switching paradigm developed by Yee et al. (2016, 2019). On each trial a letter-number pair was visually presented (e.g., one letter and one number on the screen), and participants were tasked with categorizing the target symbol based on the task instruction briefly presented at the beginning of each trial (e.g., classify the letter was a vowel or consonant, the number as odd or even). Participants maintained both task rules in working memory, and the task for a given trial was indicated by a cue display, which was randomized across trials and preceded the number-letter pair, indicating either "Attend Letter" or "Attend Number". A reward cue was placed above and below each task instruction, which indicated a low, medium, or high reward value (displayed as "$", "$$", or "$$$$"). The values of the monetary reward cues were randomized across trials. Although reward cues were always presented with task cues, participants could only earn monetary reward during incentive blocks (i.e., not during practice and baseline blocks).

During the incentive blocks, participants could earn monetary rewards for fast and accurate task performance (See Procedure). A key aspect of the experimental design was the utilization of monetary reward cues that varied on a trial-by-trial basis. Successful attainment of the monetary reward was indicated by oral liquid delivery to the participant's mouth as post-trial performance feedback. At the end of trials in which participants were accurate and faster than the criterion RT, they received a 1 mL drop of liquid directly to their mouths. Participants only received liquid

feedback for successfully earning monetary reward in a given trial, and did not receive liquid if they were incorrect, too slow, or did not respond. Critically, although the type of liquid received was blocked, such that the liquid feedback could be positive/appetitive (apple juice), neutral (isotonic tasteless solution), or negative/aversive (saltwater), the symbolic meaning of the liquid was kept constant. Thus, any behavioral differences observed between liquid types can be attributed to differential subjective valuation of liquid feedback, and simultaneous consideration of both monetary rewards and liquid incentives during task performance. Importantly, because receipt of both monetary reward and liquid feedback was performance-contingent, participants had to integrate the value of both incentives (i.e., motivational incentive integration) when performing the cognitive task. Thus, the task enables straightforward comparison of the parametric effects of value on task performance for each motivational incentive (e.g., low vs. medium vs. high monetary rewards), as well as for "bundled" incentives (e.g., juice + high monetary reward vs. neutral + high monetary reward) that reflect the effect of integrated motivational value on cognitive task performance.

The task was programmed with Psychtoolbox 3 (version 3.0.12) in Matlab (version 2016b) and displayed on projector connected to a laptop computer. Each trial consisted of a fixation display displayed for 300 ms, a cue display with the task instruction and monetary reward value for 500 ms, a blank display for 1850 ms, a target display of the number-letter pair for 2000 ms, a second fixation display for 1000 ms, and a feedback display for 2000 ms (See Figure 1A). Finally, an inter-trial interval of randomized duration (3000, 5000, or 7000 ms) displayed the fixation cross prior to the start of the next trial. Response mappings were counterbalanced between participants.

Procedure

Participants were asked to abstain from eating or drinking anything besides water for two hours before the start of the session. Upon arrival, participants completed a contact information questionnaire with demographic information, along with the Behavioral Inhibition & Avoidance Scales (BIS/BAS), a self-report survey often used to measure individual differences in motivation to avoid aversive outcomes and approach goal-oriented outcomes (Carver and White, 1994).

Next, participants practiced the task for 30 minutes in a testing room. They first practiced single tasks (letter categorization or number categorization only; order counterbalanced across participants), followed by practice of a mixed task block (task-switching between letter and number task rules). During the three practice blocks (one letter, one number, one mixed), participants received visual performance feedback to indicate accurate performance after each trial. During the three baseline blocks (one letter, one number, one mixed), participants no longer received performance feedback. Additionally, participants practiced swallowing the liquids while lying down on a bed in the testing room, and several drops of the neutral solution liquid was delivered via a pacifier and plastic tubing from the computer-triggered liquid delivery setup.

During scanning, a mixed block/event-related task design was used to optimize characterization of non-linear and time-sensitive neuronal responses, and to enable simultaneous extraction of trial-related transient activity and block-related sustained activity related to task-level processing (Petersen and Dubis, 2012). Each run consisted of 48 trials divided between three blocks (16 trials per block), alternating with 30 seconds of "rest" in which participants were instructed to attend a fixation cross display (See Figure 2B). Participants performed one or two baseline runs, in which they performed the task without earning incentives. Each participant's reward criterion (40%) was calculated based on their response times in the baseline runs.

Following the baseline runs, participants completed six incentive blocks with liquid delivered as performance feedback for successful attainment of monetary reward (two juice, two neutral, two saltwater). Liquid order was counterbalanced. Participants received 1 mL of liquid delivered directly to their mouths (see Liquid Setup and Delivery Procedure) if they were accurate and faster than their calculated reward criterion (40% faster than baseline performance). If participants were incorrect, too slow, or did not respond, they did not earn monetary reward and did not receive any liquid during that trial.

After completion of the scanning session, participants completed a post-task questionnaire and reported Likert ratings (1-7) of motivation of the liquids for each of the nine task conditions (See Figure 1C). Participants additionally reported Likert ratings of liking and intensity for each liquid (See Figure S1). Reward earnings were calculated and added to their base rate earnings for experimental participation.

Liquid Setup and Delivery Procedure

Prior the scan, the neutral and saltwater liquid solution were prepared in a testing room in the CCP lab. The isotonic neutral solution consisted of 1 liter of distilled water, .0495g of NaHCO3 (sodium bicarbonate), and .4668g of KCl (potassium chloride). The saltwater solution consisted of 500 mL of distilled water and 8.8g of non-iodized salt. The juice used was 100% apple juice (Mott's) and purchased from the store.

During both the behavioral practice and scanning session, the liquids were dispensed using a digital infusion pump (model SP210iw, World Precision Instruments, Inc.) triggered by an output signal from the Matlab script and delivered via Tygon tubing and a pacifier directly to the participant's mouth. The infusion pump was located in the control room, and lengthy tubing was

used to ensure that the dispensed liquid was delivered to the participants. The type of liquid delivered was manipulated in a blocked fashion, counterbalanced across participants, such that on a given block participants would receive positive / appetitive (apple juice), neutral (isotonic tasteless solution), or negative / aversive (saltwater) performance feedback.

Behavioral Data Analysis

Behavioral data were analyzed in Rstudio using the R statistical language (RStudioTeam, 2016; R Core Team, 2017). All of the data were visualized using ggplot2 package (Wickham, 2016). All of the linear mixed effects models were conducted using the lmerTest (Kuznetsova, Brockoff and Christensen, 2015) and LME4 (Bates *et al.*, 2015) packages in RStudio using the R statistical language (RStudioTeam, 2016; R Core Team, 2017). When applicable, confidence intervals for the effects were calculated using the "confint" function in the lme4 package. The Bayesian multilevel mediation analyses was conducted using the bmlm package in R (Vuorre and Bolger, 2018). The knitr and Rmarkdown packages were used to create dynamic reports of the results (Xie, 2019).

fMRI Data Acquisition and Preprocessing

MRI data were acquired on a 3-Tesla Siemens Trio scanner equipped with a 32-channel head coil. A T1-weighed MPRAGE scan was acquired for each participant (TR = 2400 ms, TE =3.16 ms, Flip angle = 8 degrees, 64 slices, slice thickness = 1.0 mm, FOV = 256 x 256 mm). For each EPI bold run (1 or 2 baseline, 6 incentive), 360 volumes were acquired with 4 mm isotropic voxels (TR = 2000 ms, TE = 30.0 ms, Flip angle = 77 degrees, 32 slices, interleaved order, slice

thickness=4 mm, FOV = 384×384 mm, acquisition matrix 64×64 yielding an in-plane resolution of 4×4 mm).

Preprocessing for both anatomical and functional data was performed using fMRIPrep version 1.1.7 (Esteban *et al.*, 2019), which is based on Nipype version 1.1.3 (Gorgolewski *et al.*, 2011). The T1-weighted (T1w) image was corrected for intensity non-uniformity (INU) using N4BiasFieldCorrection (ANTs 2.2.0) (Tustison *et al.*, 2010), and used as T1w-reference throughout the workflow. The T1w-reference was then skull-stripped using antsBrainExtraction.sh (ANTs 2.2.0), using OASIS as target template. Brain surfaces were reconstructed using recon-all (FreeSurfer 6.0.1) (Dale, Fischl and Sereno, 1999), and the brain mask estimated previously was refined with a custom variation of the method to reconcile ANTs-derived and FreeSurfer-derived segmentations of the cortical gray-matter of Mindboggle (Klein *et al.*, 2017). Spatial normalization to the ICBM 152 Nonlinear Asymmetrical template version 2009c (Fonov *et al.*, 2011) was performed through nonlinear registration with antsRegistration (ANTs 2.2.0) (Avants *et al.*, 2008), using brain-extracted versions of both T1w volume and template. Brain tissue segmentation of cerebrospinal fluid (CSF), white-matter (WM) and gray-matter (GM) was performed on the brain-extracted T1w using fast (FSL 5.0.9) (Zhang, Brady and Smith, 2001).

For each of the 8 BOLD EPI runs per participant (across all tasks and sessions), the following preprocessing was performed. First, a reference volume and its skull-stripped version were generated using the custom methodology of fMRIPrep. The BOLD reference was then co-registered to the T1w reference using bbregister (FreeSurfer) which implements boundary-based registration (Greve and Fischl, 2009). Co-registration was configured with nine degrees of freedom to account for distortions remaining in the BOLD reference. Head-motion parameters with respect to the BOLD reference (transformation matrices, and six corresponding rotation and translation

parameters) were estimated before any spatiotemporal filtering using mcflirt (FSL 5.0.9) (Jenkinson *et al.*, 2002). BOLD runs were slice-time corrected using 3dTshift from AFNI (Cox, 1996; Cox and Hyde, 1997). The BOLD time-series (including slice-timing correction when applied) were resampled onto their original, native space by applying a single, composite transform to correct for head-motion and susceptibility distortions. These resampled BOLD time-series will be referred to as preprocessed BOLD in original space, or just preprocessed BOLD. The BOLD time-series were resampled to MNI152NLin2009cAsym standard space, generating a preprocessed BOLD run in MNI152NLin2009cAsym space. Several confounding time-series were calculated based on the preprocessed BOLD: framewise displacement (FD), DVARS and three region-wise global signals. FD and DVARS are calculated for each functional run, both using their implementations in Nipype (following the definitions by (Power *et al.*, 2014)). The head-motion estimates calculated in the correction step were also placed within the corresponding confounds file. The BOLD time-series were resampled to surfaces on the following spaces: fsaverage. All resamplings were performed with a single interpolation step by composing all the pertinent transformations (i.e. head-motion transform matrices, susceptibility distortion correction when available, and co-registrations to anatomical and template spaces). Gridded (volumetric) resamplings were performed using antsApplyTransforms (ANTs), configured with Lanczos interpolation to minimize the smoothing effects of other kernels (Lanczos, 1964). Non-gridded (surface) resamplings were performed using mri_vol2surf (FreeSurfer).

Next, the preprocessed BOLD runs were smoothed with a 4 mm FWHM kernel using 3dBlurtoFWHM from AFNI, as well as scaling (voxels were demeaned) using 3dTstat and 3dcalc from AFNI. Finally, the images were reoriented to LPI orientation using AFNI's 3dresample function.

fMRI Data Analysis

To optimize analyses for the mixed block/event-related task design (Visscher *et al.*, 2003; Petersen and Dubis, 2012), a general linear model (GLM) was applied to extract beta estimates and t-statistics for both the sustained liquid block conditions and the transient event-related motivational conditions for each participant. Specifically, AFNI's 3dDeconvolve function was used to set up the GLM and build an input matrix with the hemodynamic regression model, which contains the duration modulated block effects (dmblock) for baseline, juice, neutral, and saltwater runs, as well as a parameter tent function expansion for every two seconds between 0 and 24 seconds after the onset of the cue stimulus (TENTzero) for each of the 9 motivation conditions (3 levels of money, 3 levels of liquid, rewarded trials only), and unrewarded trials. The TENTzero function eliminates the first and last basis functions from the set, forcing the deconvolved hemodynamic response function (HRF) to be zero at the start and end of the response window. Importantly, this function enables modeling the HRF without assuming a specific shape for the hemodynamic response (e.g., gamma). Such an estimation approach is advantageous for the complex multi-event (i.e., cue, delay, target, feedback) trials employed here.

The GLM was run with 3dREMLfit from AFNI, which performs a generalized least squares time series regression (aka 'prewhitened' least squares) combined with a restricted maximum likelihood (REML) estimation of an Autoregressive Moving Average Model (ARMA(1,1)) temporal correlation structure, which has been argued to substantially improve reliability in task fMRI studies (Olszowy *et al.*, 2019). For each participant, we computed whole brain beta estimates for the 4 block types (baseline, juice, neutral, saltwater), 9 tent functions for each of the motivation conditions (3 monetary reward levels x 3 liquid types) (See Equation). A tent function regressor for incorrect trials and the six motion parameters generated from fMRIPrep

realignment were included in the GLM as nuisance regressors. Additionally, TRs were censored (current and previous) if the derivative values were estimated (in fMRIPrep) to have a Euclidean norm above .9 mm.

$$\boldsymbol{BOLD} = \boldsymbol{X}\beta_{\text{B_Baseline}} + \boldsymbol{X}\beta_{\text{B_Juice}} + \boldsymbol{X}\beta_{\text{B_Neut}} + \boldsymbol{X}\beta_{\text{B_Salt}} + \boldsymbol{X}\beta_{\text{EV1_Juice}} + \boldsymbol{X}\beta_{\text{EV2_Juice}} + \boldsymbol{X}\beta_{\text{EV4_Juice}} + \boldsymbol{X}\beta_{\text{EV1_Neut}} + \boldsymbol{X}\beta_{\text{EV2_Neut}} + \boldsymbol{X}\beta_{\text{EV4_Neut}} + \boldsymbol{X}\beta_{\text{EV1_Salt}} + \boldsymbol{X}\beta_{\text{EV2_Salt}} + \boldsymbol{X}\beta_{\text{EV4_Salt}} + \varepsilon$$

Next, these mixed block/event-related beta estimates were extracted for each of the 400 parcels from the Schaefer cortical atlas, divided into 7 functional networks (Schaefer *et al.*, 2017). The Schaefer atlas was selected because its approach of using a gradient-weighted Markov Random Field to integrate local gradient and global similarity metrics across resting state fMRI and task-based fMRI acquisition protocols yielded the most homogenous parcellations and thus correspond with higher precision to cortical areas compared to prior parcellation schemes (Yeo *et al.*, 2011; Gordon *et al.*, 2016). Additionally, given our a priori hypotheses in subcortical regions, beta estimates were calculated for 19 subcortical regions of interest (ROIs) that were anatomically defined from Freesurfer. Beta estimates were averaged for all voxels within each parcel using 3dROIstats from AFNI.

For the dACC ROI analyses, five parcels from the Schaefer cortical parcellation scheme (400 parcels, 7 networks, 2 mm voxels) were identified and averaged, using criteria that were conservative and anatomically focused in corresponding to bilateral dACC based upon a prior meta-analysis on motivated cognitive control (Parro, Dixon and Christoff, 2018). Specifically, the following parcels were included in bilateral dACC: 107 (‘LH_SalVentAttn_Med_1), 108 (‘LH_SalVentAttn_Med_2’), 110 (‘LH_SalVentAttn_Med_3), 311 (‘RH_SalVentAttn_Med_1’),

312 (‘RH_ SalVentAttn_Med_2’). MNI coordinates of these five parcels corresponding to dACC are listed in the table below[b].

Table 1: Parcels included in Bilateral Dorsal ACC ROI Mask.

Parcel ID	**Parcel Number**	**MNI Coordinates (RAS)**		
		x	y	z
107	LH_SalVentAttn_Med_1	-6	22	32
108	LH_SalVentAttn_Med_2	-6	0	40
110	LH_SalVentAttn_Med_3	-6	10	48
311	RH_SalVentAttn_Med_1	8	18	26
312	RH_SalVentAttn_Med_2	8	2	42

[b]All coordinates for the Schaefer parcellation scheme can be found on the YeoLab Github link: https://github.com/ThomasYeoLab/CBIG/blob/master/stable_projects/brain_parcellation/Schaefer2018_LocalGlobal/Parcellations/MNI/Centroid_coordinates/

References

Avants, B. B. *et al.* (2008) 'Symmetric diffeomorphic image registration with cross-correlation : Evaluating automated labeling of elderly and neurodegenerative brain', *Medical Image Analysis*, 12, pp. 26–41. doi: 10.1016/j.media.2007.06.004.

Bahlmann, J., Aarts, E. and D'Esposito, M. (2015) 'Influence of Motivation on Control Hierarchy in the Human Frontal Cortex', *Journal of Neuroscience*, 35(7), pp. 3207–3217. doi: 10.1523/JNEUROSCI.2389-14.2015.

Balleine, B. W., Delgado, M. R. and Hikosaka, O. (2007) 'The Role of the Dorsal Striatum in Reward and Decision-Making', *Journal of Neuroscience*, 27(31), pp. 8161–8165. doi: 10.1523/JNEUROSCI.1554-07.2007.

Balleine, B. W. and O'Doherty, J. P. (2010) 'Human and rodent homologies in action control: corticostriatal determinants of goal-directed and habitual action.', *Neuropsychopharmacology : official publication of the American College of Neuropsychopharmacology*, 35(1), pp. 48–69. doi: 10.1038/npp.2009.131.

Bartra, O., McGuire, J. T. and Kable, J. W. (2013) 'The valuation system: A coordinate-based meta-analysis of BOLD fMRI experiments examining neural correlates of subjective value', *NeuroImage*. Elsevier Inc., 76, pp. 412–427. doi: 10.1016/j.neuroimage.2013.02.063.

Bates, D. M. *et al.* (2015) 'Linear mixed-effects models using Eigen and S4'. R package version (2015). Available at: http://cran.r-project.org/web/packages/lme4/lme4.pdf.

Bonner, S. E. and Sprinkle, G. B. (2002) 'The effects of monetary incentives on effort and task performance: Theories, evidence, and a framework for research', *Accounting, Organizations and Society*, 27(4–5), pp. 303–345. doi: 10.1016/S0361-3682(01)00052-6.

Botvinick, M. M. and Braver, T. S. (2015) 'Motivation and Cognitive Control: From Behavior to Neural Mechanism', *Annual review of psychology*, 66, pp. 83–113. doi: 10.1146/annurev-psych-010814-015044.

Bush, G. *et al.* (2002) 'Dorsal anterior cingulate cortex: a role in reward-based decision making.', *Proceedings of the National Academy of Sciences of the United States of America*, 99(1), pp. 523–8. doi: 10.1073/pnas.012470999.

Cai, X. and Padoa-Schioppa, C. (2012) 'Neuronal encoding of subjective value in dorsal and ventral anterior cingulate cortex', *Journal of Neuroscience*, 32(11), pp. 3791–3808. doi: 10.1523/JNEUROSCI.3864-11.2012.

Camille, N., Tsuchida, A. and Fellows, L. K. (2011) 'Double dissociation of stimulus-value and action-value learning in humans with orbitofrontal or anterior cingulate cortex damage', *Journal of Neuroscience*, 31(42), pp. 15048–15052. doi: 10.1523/JNEUROSCI.3164-11.2011.

Carver, C. S. and White, T. L. (1994) 'Behavioral inhibition, behavioral activation, and affective responses to impending reward and punishment: The BIS/BAS Scales.', *Journal of Personality and Social Psychology*, 67(2), pp. 319–333. doi: 10.1037//0022-3514.67.2.319.

Chib, V. S. *et al.* (2009) 'Evidence for a common representation of decision values for dissimilar goods in human ventromedial prefrontal cortex.', *The Journal of Neuroscience*, 29(39), pp. 12315–20. doi: 10.1523/JNEUROSCI.2575-09.2009.

Cox, R. (1996) 'AFNI : Software for Analysis and Visualization of Functional Magnetic Resonance Neuroimages', *Computers and Biomedical Research*, 29, pp. 162–173.

Cox, R. W. and Hyde, J. S. (1997) 'Software Tools for Analysis and Visualization of fMRI Data', *NMR in Biomedicine*, 10, pp. 171–178.

Crawford, J. L. *et al.* (2020) 'Dissociable Effects of Monetary , Liquid , and Social Incentives on Motivation and Cognitive Control', *Frontiers in Psychology*, 11(September), pp. 1–14. doi: 10.3389/fpsyg.2020.02212.

Croxson, P. L. *et al.* (2009) 'Effort-based cost-benefit valuation and the human brain.', *The Journal of Neuroscience*, 29(14), pp. 4531–41. doi: 10.1523/JNEUROSCI.4515-08.2009.

Dale, A. M., Fischl, B. and Sereno, M. I. (1999) 'Cortical Surface-Based Analysis', *Neuroimage*, 9, pp. 179–194.

Dang, J., King, K. M. and Inzlicht, M. (2020) 'Why Are Self-Report and Behavioral Measures Weakly Correlated?', *Trends in Cognitive Sciences*. Elsevier Ltd, 24(4), pp. 267–269. doi: 10.1016/j.tics.2020.01.007.

Dixon, M. L. and Christoff, K. (2012) 'The Decision to Engage Cognitive Control Is Driven by Expected Reward-Value: Neural and Behavioral Evidence', *PLoS ONE*, 7(12). doi: 10.1371/journal.pone.0051637.

Duverne, S. and Koechlin, E. (2017) 'Rewards and Cognitive Control in the Human Prefrontal Cortex', *Cerebral Cortex*, (September), pp. 1–16. doi: 10.1093/cercor/bhx210.

Esteban, O. *et al.* (2019) 'fMRIPrep: a robust preprocessing pipeline for functional MRI', *Nature Methods*. Springer US, 16(January). doi: 10.1038/s41592-018-0235-4.

Etzel, J. *et al.* (2015) 'Reward motivation enhances task representation coding in frontoparietal cortex', *Cerebral cortex (New York, N.Y. : 1991)*, pp. 1–13. doi: 10.1093/cercor/bhu327.

FitzGerald, T. H. B., Seymour, B. and Dolan, R. J. (2009) 'The role of human orbitofrontal cortex in value comparison for incommensurable objects.', *The Journal of Neuroscience*, 29(26), pp. 8388–8395. doi: 10.1523/JNEUROSCI.0717-09.2009.

Fonov, V. *et al.* (2011) 'NeuroImage Unbiased average age-appropriate atlases for pediatric

studies', *NeuroImage*. Elsevier Inc., 54(1), pp. 313–327. doi: 10.1016/j.neuroimage.2010.07.033.

Frömer, R., Wolf, C. K. D. and Shenhav, A. (2019) 'Goal congruency dominates reward value in accounting for behavioral and neural correlates of value-based decision-making', *Nature Communications*. Springer US, 10(4926). doi: https://doi.org/10.1038/s41467-019-12931-x.

Fujiwara, J. *et al.* (2009) 'Segregated and integrated coding of reward and punishment in the cingulate cortex.', *Journal of neurophysiology*, 101(6), pp. 3284–3293. doi: 10.1152/jn.90909.2008.

Gordon, E. M. *et al.* (2016) 'Generation and Evaluation of a Cortical Area Parcellation from Resting-State Correlations', *Cerebral Cortex*, 26(1), pp. 288–303. doi: 10.1093/cercor/bhu239.

Gorgolewski, K. *et al.* (2011) 'Nipype: a flexible, lightweight and extensible neuroimaging data processing framework in Python', *Frontiers in Neuroinformatics*, 5(August), pp. 1–15. doi: 10.3389/fninf.2011.00013.

Grahek, I. *et al.* (2019) 'Motivation and cognitive control in depression', *Neuroscience and Biobehavioral Reviews*. Elsevier, 102(April), pp. 371–381. doi: 10.1016/j.neubiorev.2019.04.011.

Greve, D. N. and Fischl, B. (2009) 'NeuroImage Accurate and robust brain image alignment using boundary-based registration', *NeuroImage*. Elsevier Inc., 48(1), pp. 63–72. doi: 10.1016/j.neuroimage.2009.06.060.

Harris, P. *et al.* (2009) 'Research electronic data capture (REDCap)-A metadata-driven methodology and workflow process for providing translational research informatics support', *Journal of Biomedical Informatics*. Elsevier Inc., 42(2), pp. 377–381. doi: 10.1016/j.jbi.2008.08.010.

Hayden, B. Y. and Platt, M. L. (2010) 'Neurons in anterior cingulate cortex multiplex information about reward and action', *Journal of Neuroscience*, 30(9), pp. 3339–3346. doi: 10.1523/JNEUROSCI.4874-09.2010.

Heilbronner, S. R. and Hayden, B. Y. (2016) 'Dorsal Anterior Cingulate Cortex: A Bottom-Up View', *Annual Review of Neuroscience*, 39(1), pp. 149–170. doi: 10.1146/annurev-neuro-070815-013952.

Hermans, H. J. (1970) 'A questionnaire measure of achievement motivation', *Journal of Applied Psychology*, 54(4), pp. 353–363. doi: 10.1037/h0029675.

Holroyd, C. B. and McClure, S. M. (2015) 'Hierarchical control over effortful behavior by rodent medial frontal cortex: A computational model.', *Psychological Review*, 122(1), pp. 54–83. doi: 10.1037/a0038339.

Holroyd, C. B. and Yeung, N. (2011) 'An integrative theory of anterior cingulate cortex

function: Option selection in hierarchical reinforcement learning', in *The Neural Basis of Motivational and Cognitive Control*. Cambridge, Massachusetts: MIT Press, pp. 333–349.

Holroyd, C. B. and Yeung, N. (2012) 'Motivation of extended behaviors by anterior cingulate cortex', *Trends in Cognitive Sciences*. Elsevier Ltd, 16(2), pp. 122–128. doi: 10.1016/j.tics.2011.12.008.

Hosking, J. G., Cocker, P. J. and Winstanley, C. A. (2014) 'Dissociable contributions of anterior cingulate cortex and basolateral amygdala on a rodent cost/benefit decision-making task of cognitive effort', *Neuropsychopharmacology*. Nature Publishing Group, 39(7), pp. 1558–1567. doi: 10.1038/npp.2014.27.

Huang, H. *et al.* (2015) 'The influence of depression on cognitive control: Disambiguating approach and avoidance tendencies', *PLoS ONE*, 10(11), pp. 1–13. doi: 10.1371/journal.pone.0143714.

Jenkinson, M. *et al.* (2002) 'Improved Optimization for the Robust and Accurate Linear Registration and Motion Correction of Brain Images', *NeuroImage*, 841, pp. 825–841. doi: 10.1006/nimg.2002.1132.

Kim, H., Shimojo, S. and O'Doherty, J. P. (2011) 'Overlapping responses for the expectation of juice and money rewards in human ventromedial prefrontal cortex.', *Cerebral cortex (New York, N.Y. : 1991)*, 21(4), pp. 769–76. doi: 10.1093/cercor/bhq145.

Klein-Flügge, M. C. *et al.* (2016) 'Neural signatures of value comparison in human cingulate cortex during decisions requiring an effort-reward trade-off', *Journal of Neuroscience*, 36(39), pp. 10002–10015. doi: 10.1523/JNEUROSCI.0292-16.2016.

Klein, A. *et al.* (2017) 'Mindboggling morphometry of human brains', pp. 1–40. doi: 10.1371/journal.pcbi.1005350.

Kolling, N. *et al.* (2016) 'Value, search, persistence and model updating in anterior cingulate cortex', *Nature Neuroscience*, 19(10), pp. 1280–1285. doi: 10.1038/nn.4382.

Kouneiher, F., Charron, S. and Koechlin, E. (2009) 'Motivation and cognitive control in the human prefrontal cortex.', *Nature neuroscience*, 12(7), pp. 939–45. doi: 10.1038/nn.2321.

Krug, M. and Braver, T. S. (2014) 'Motivation and Cognitive Control: Going Beyond Monetary Incentives', in *The Psychological Science of Money*, pp. 137–158. doi: 10.1007/978-1-4939-0959-9_10.

Kuznetsova, A., Brockoff, P. B. and Christensen, R. H. (2015) 'lmerTest: Tests for random and fixed effects for linear mixed effect models (lmer objects of lme4 package)'. R package version (2015). Available at: http://cran.r-project.org/web/packages/lmerTest/lmerTest.pdf.

Lake, J. I. *et al.* (2019) 'Reward anticipation and punishment anticipation are instantiated in the

brain via opponent mechanisms', *Psychophysiology*, (March), pp. 1–14. doi: 10.1111/psyp.13381.

Lanczos, C. (1964) 'Evaluation of Noisy Data', *Journal of the Society for Industrial and Applied Mathematics: Series B, Numerical Analysis*, 1, pp. 76–85. Available at: https://www.jstor.org/stable/2949766.

Lehner, R. *et al.* (2017) 'Monetary, Food, and Social Rewards Induce Similar Pavlovian-to-Instrumental Transfer Effects', *Frontiers in Behavioral Neuroscience*, 10(January), pp. 1–12. doi: 10.3389/fnbeh.2016.00247.

Levy, D. J. and Glimcher, P. W. (2012) 'The root of all value: a neural common currency for choice.', *Current opinion in neurobiology*. Elsevier Ltd, 22(6), pp. 1027–38. doi: 10.1016/j.conb.2012.06.001.

Miller, E. M. *et al.* (2014) 'Dissociating Motivation from Reward in Human Striatal Activity', *Journal of Cognitive Neuroscience*, 26(5), pp. 1075–1084. doi: 10.1162/jocn_a_00535.

Monosov, I. E. (2017) 'Anterior cingulate is a source of valence-specific information about value and uncertainty', *Nature Communications*. Springer US, 8(34), pp. 1–11. doi: 10.1038/s41467-017-00072-y.

Olszowy, W. *et al.* (2019) 'Accurate autocorrelation modeling substnatially improves fMRI reliability', *Nature Communications*. Springer US, pp. 1–11. doi: 10.1038/s41467-019-09230-w.

Padmala, S. and Pessoa, L. (2011) 'Reward Reduces Conflict by Enhancing Attentional Control and Biasing Visual Cortical Processing', *Journal of Cognitive Neuroscience*, 23(11), pp. 3419–3432. doi: 10.1162/jocn_a_00011.

Padoa-Schioppa, C. (2011) 'Neurobiology of Economic Choice : A Good-Based Model', *Annual Review of Neuroscience*, 34, pp. 333–359. doi: 10.1146/annurev-neuro-061010-113648.

Padoa-Schioppa, C. and Conen, K. E. (2017) 'Orbitofrontal Cortex: A Neural Circuit for Economic Decisions', *Neuron*. Elsevier Inc., 96(4), pp. 736–754. doi: 10.1016/j.neuron.2017.09.031.

Park, H. R. P. *et al.* (2018) 'Smiling faces and cash bonuses: Exploring common affective coding across positive and negative emotional and motivational stimuli using fMRI', *Cognitive, Affective and Behavioral Neuroscience*. Cognitive, Affective, & Behavioral Neuroscience, 18(3), pp. 550–563. doi: 10.3758/s13415-018-0587-3.

Park, S. Q. *et al.* (2011) 'Neurobiology of value integration: when value impacts valuation.', *The Journal of Neuroscience*, 31(25), pp. 9307–9314. doi: 10.1523/JNEUROSCI.4973-10.2011.

Parro, C., Dixon, M. L. and Christoff, K. (2018) 'The neural basis of motivational influences on cognitive control', *Human Brain Mapping*, 39, pp. 5097–5111. doi: 10.1002/hbm.24348.

Peters, J. and Büchel, C. (2010) 'Neural representations of subjective reward value.', *Behavioural brain research*, 213(2), pp. 135–41. doi: 10.1016/j.bbr.2010.04.031.

Petersen, S. E. and Dubis, J. W. (2012) 'The mixed block/event-related design', *NeuroImage*. Elsevier Inc., 62(2), pp. 1177–1184. doi: 10.1016/j.neuroimage.2011.09.084.

Power, J. D. *et al.* (2014) 'NeuroImage Methods to detect , characterize , and remove motion artifact in resting state fMRI', *NeuroImage*. Elsevier Inc., 84, pp. 320–341. doi: 10.1016/j.neuroimage.2013.08.048.

R Core Team (2017) 'R: A language for statistical computing'. Vienna, Austria: R Foundation for Statistical Computing.

RStudioTeam (2016) 'RStudio: Integrated Development for R.' Boston, MA: Rstudio, Inc. Available at: http://www.rstudio.com/.

Rushworth, M. F. S. *et al.* (2004) 'Action sets and decisions in the medial frontal cortex', *Trends in Cognitive Sciences*, 8(9), pp. 410–417. doi: 10.1016/j.tics.2004.07.009.

Sayalı, C. and Badre, D. (2019) 'Neural systems of cognitive demand avoidance', *Neuropsychologia*. Elsevier Ltd, 123(October 2017), pp. 41–54. doi: 10.1016/j.neuropsychologia.2018.06.016.

Schaefer, A. *et al.* (2017) 'Local-Global Parcellation of the Human Cerebral Cortex from Intrinsic Functional Connectivity MRI', *Cerebral Cortex*, (September), pp. 1–20. doi: 10.1093/cercor/bhx179.

Schneider, K. N. *et al.* (2020) 'Anterior Cingulate Cortex Signals Attention in a Social Paradigm that Manipulates Reward and Shock', *Current Biology*. Elsevier Ltd., pp. 1–12. doi: 10.1016/j.cub.2020.07.039.

Sescousse, G. *et al.* (2013) 'Processing of primary and secondary rewards: a quantitative meta-analysis and review of human functional neuroimaging studies.', *Neuroscience and biobehavioral reviews*. Elsevier Ltd, 37(4), pp. 681–96. doi: 10.1016/j.neubiorev.2013.02.002.

Sescousse, G., Li, Y. and Dreher, J. C. (2015) 'A common currency for the computation of motivational values in the human striatum', *Social Cognitive and Affective Neuroscience*, 10(4), pp. 467–473. doi: 10.1093/scan/nsu074.

Shenhav, A. *et al.* (2017) 'Toward a Rational and Mechanistic Account of Mental Effort', *Annual Review of Neuroscience*, 40(1), pp. 99–124. doi: 10.1146/annurev-neuro-072116-031526.

Shenhav, A., Botvinick, M. M. and Cohen, J. D. (2013) 'The expected value of control: an integrative theory of anterior cingulate cortex function.', *Neuron*. Elsevier Inc., 79(2), pp. 217–40. doi: 10.1016/j.neuron.2013.07.007.

Shenhav, A., Cohen, J. D. and Botvinick, M. M. (2016) 'Dorsal anterior cingulate cortex and the value of control', *Nature Neuroscience*, 19(10), pp. 1280–1285. doi: 10.1038/nn.4382.

Small, D. M. (2010) 'Taste representation in the human insula', *Brain Structure and Function*, 214, pp. 551–561. doi: 10.1007/s00429-010-0266-9.

Tustison, N. J. *et al.* (2010) 'N4ITK: Improved N3 Bias Correction', *IEEE Transactions on Medical Imaging*, 29(6), pp. 1310–1320.

Vega, A. De *et al.* (2016) 'Large-Scale Meta-Analysis of Human Medial Frontal Cortex Reveals Tripartite Functional Organization', *Journal of Neuroscience*, 36(24), pp. 6553–6562. doi: 10.1523/JNEUROSCI.4402-15.2016.

Visscher, K. M. *et al.* (2003) 'Mixed blocked/event-related designs separate transient and sustained activity in fMRI', *NeuroImage*, 19, pp. 1694–1708. doi: 10.1016/S1053-8119(03)00178-2.

Vuorre, M. and Bolger, N. (2018) 'Within-subject mediation analysis for experimental data in cognitive psychology and neuroscience', *Behavior Research Methods*. Behavior Research Methods, 50(5), pp. 2125–2143. doi: 10.3758/s13428-017-0980-9.

Westbrook, A., Lamichhane, B. and Braver, T. (2019) 'The Subjective Value of Cognitive Effort is Encoded by a Domain-General Valuation Network', *Journal of Neuroscience*, 39(20), pp. 3934–3947.

Wickham, H. (2016) 'ggplot2: Elegant Graphics for Data Analysis', in. Springer-Verlag New York.

Wisniewski, D. *et al.* (2015) 'The Role of the Parietal Cortex in the Representation of Task-Reward Associations', *Journal of Neuroscience*, 35(36), pp. 12355–12365. doi: 10.1523/JNEUROSCI.4882-14.2015.

Xie, Y. (2019) 'knitr: A General-Purpose Package for Dynamic Report Generation in R', R package.

Yee, D. M. *et al.* (2016) 'Humans Integrate Monetary and Liquid Incentives to Motivate Cognitive Task Performance', *Frontiers in Psychology*, 6(January), pp. 1–17. doi: 10.3389/fpsyg.2015.02037.

Yee, D. M. *et al.* (2019) 'Age-Related Differences in Motivational Integration and Cognitive Control', *Cognitive, Affective, & Behavioral Neuroscience*. Cognitive, Affective, & Behavioral Neuroscience, 19, pp. 692–714.

Yee, D. M. and Braver, T. S. (2018) 'Interactions of motivation and cognitive control', *Current Opinion in Behavioral Sciences*. Elsevier Ltd, 19, pp. 83–90. doi: 10.1016/j.cobeha.2017.11.009.

Yeo, B. T. T. *et al.* (2011) 'The organization of the human cerebral cortex estimated by intrinsic functional connectivity', *Journal of Neurophysiology*, 106, pp. 1125–1165. doi: 10.1152/jn.00338.2011.

Zhang, Y., Brady, M. and Smith, S. (2001) 'Segmentation of Brain MR Images Through a Hidden Markov Random Field Model and the Expectation-Maximization Algorithm', *IEEE Transactions on Medical Imaging*, 20(1), pp. 45–57.

Zhang, Z. *et al.* (2017) 'Distributed neural representation of saliency controlled value and category during anticipation of rewards and punishments', *Nature Communications*. Springer US, 8(1), p. 1907. doi: 10.1038/s41467-017-02080-4.